Doubly dressed states in a ladder-type system with electromagnetically induced transparency

Ray-Yuan Chang, Wei-Chia Fang, Zong-Syun He, Bai-Cian Ke, Pei-Ning Chen, and Chin-Chun Tsai*
Department of Physics, National Cheng Kung University, Tainan, Taiwan 70101
(Received 24 August 2007; published 28 November 2007)

Doubly dressed states in a ladder-type two-photon, three-level coupling system are observed. The electromagnetically induced transparency (EIT) doublet signal is interpreted as arising from the absorption and gain components of the Mollow spectrum. The separation of the EIT doublet matches the theoretical prediction. A numerical simulation demonstrates that the Doppler velocity group may perturb the light shift from the symmetric center of the EIT doublet. The quantum nature of the EIT system significantly suppresses Doppler broadening.

DOI: 10.1103/PhysRevA.76.053420 PACS number(s): 32.80.Qk, 03.67.Lx, 42.50.Gy

I. INTRODUCTION

The dressed state picture of a system of atom-photon interactions has been extensively studied [1]. The simplest atom-photon interaction is the two-level system that is coupled by one coherent field. A theoretical description was presented and experimental observations made before the dressed state picture was presented [2,3]. The three-level system coupled by two photon fields is associated with a nonlinear mechanism which is known as the Autler-Townes doublet [4], coherent population trapping [5,6], or electromagnetically induced transparency (EIT) [7]. Applications of coherent superposition among the quantum states generated from such interactions have seen numerous breakthroughs over past decades [8]. One transition pathway can be regarded as a "turning knob," mediated by the atomic coherence, that interferes with the other pathway. The ability to modify greatly either the real or the imaginary part of the transition susceptibility using this knob has attracted considerable attention in a variety of fields in physics, including the cooling of atoms below the photon recoil limit [9], lasing without population inversion [10], and the realization of highly accurate clocks [11]. Coherence effects such as two-photon inhibition and enhancement [12], evolution of double dark states [13], photon switching [14], and Kerr nonlinearity [15] have been exhibited. Additionally, along with advances in laser cooling and trapping, the dressed state picture has been very helpful in the interpretation of polarization gradient cooling [16]. Other applications of the dressed state approach, such as recoil-induced resonance [17], collective atomic recoil lasing [18,19], the velocimetry of cold atoms [20], superradiant Rayleigh scattering, and Bragg scattering in the Bose-Einstein condensate [21] have been demonstrated to be important in investigating physics of the dressed state approach. Beyond the fascinating physics of the three-level system, the dressed states can be further perturbed by an additional field to drive the dressed states coherently to a fourth state, which can be called a double dark state [22,23]. However, when both fields are sufficiently strong, and one is far detuned, the atom-photon interaction can also create the doubly dressed state under the two-photon, three-level coupling scheme. This work presents observations of a simultaneous Mollow spectrum and EIT under a ladder-type configuration. The experimental studies involve three atomic cesium eigenstates with allowed electromagnetic coupling between the lower- and upper-level pairs. Consider the three-level ladder system shown in Fig. 1, where we neglect the interparticle collision and assume the system to be closed. Atoms are driven by two coherent fields, each nearly stepwise resonant with one of two allowed transitions. The pump field drives the lower-pair $|1\rangle \leftrightarrow |2\rangle$ transition with Rabi frequency Ω_p at frequency ω_p, and the coupling field drives the transition $|2\rangle \leftrightarrow |3\rangle$ with Rabi frequency Ω_c at frequency ω_c. Let Δ_p be the pump field detuning with respect to the $|1\rangle \leftrightarrow |2\rangle$ transition, and Δ_c be the coupling field detuning of the $|2\rangle \leftrightarrow |3\rangle$ transition. The decay rates of the intermediate state $|2\rangle$ and excited state $|3\rangle$ are denoted as Γ_2 and Γ_3, which are 5.22 and 2.18 MHz, respectively. The stationary and transient behavior of the system can be well described and the steady-state solution of the pump beam absorption profile presented explicitly under the weak pump strength approximation [24]:

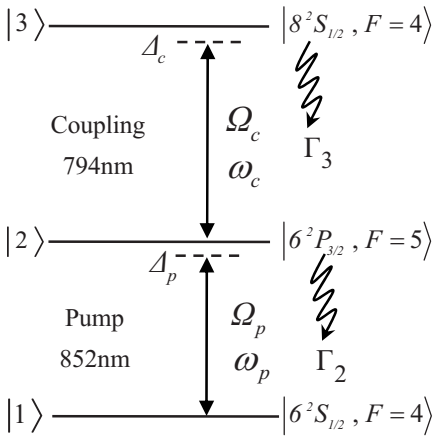

FIG. 1. Relevant energy diagram of the ladder-type three-level system of ^{133}Cs. $\Omega_{(p,c)}$, $\omega_{(p,c)}$, and $\Delta_{(p,c)}$ denote the Rabi frequency, the laser frequency, and the detuning of the pump and coupling fields. Γ_2 and Γ_3 describe the decay rate of the states $|6\,^2P_{3/2}, F=5\rangle$ and $|8\,^2S_{1/2}, F=4\rangle$, respectively.

*Corresponding author. chintsai@mail.ncku.edu.tw

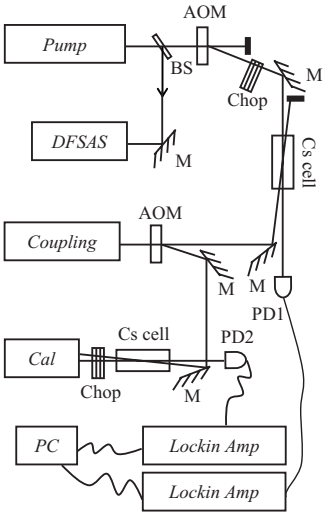

FIG. 2. Schematic diagram of the experimental setup. Coupling: The coupling laser. Pump: The pump laser, which is frequency stabilized to a hyperfine transition of the Cs cell (DFSAS). AOM: Acousto-optical modulator, serving as frequency shifter. Cal: The calibration injection-locked laser. PD(1,2): Photodetectors associated with the transimpedance amplifier. BS, beam splitter; M, mirror; chop, mechanical chopper; lock-in amp, lock-in amplifier; PC, personal computer.

$$\rho_{21} = \frac{-i\Omega_p/2}{\frac{\Gamma_2}{2} - i\Delta_p + \frac{(\Omega_c/2)^2}{\Gamma_3/2 - i(\Delta_p + \Delta_c)}}. \tag{1}$$

Notably, in the above formula, the strong coupling strongly drives the upper transition, and dressed states are formed with the superposition of the states $|2\rangle$ and $|3\rangle$. Then, the system evolves into the enhanced absorption regime as the pump field strength increases gradually, finally exceeding the effective excited state decay rate, such that the pump field further dresses the lower transition. Theoretically, this evolution is associated with the pump strength's higher-order terms becoming dominant. In the limit $\Delta_p \gg \Omega_p \gg \Gamma_2$ [17], the lower transition is greatly dressed because the ac Stark splitting is governed by

$$\sqrt{\Delta_p^2 + \Omega_p^2}. \tag{2}$$

When both of the transitions are strongly dressed, Eq. (1) fails to characterize the absorption profile, and a comprehensive picture is given using the dressed state approach for our experiment. That is conducted herein.

II. EXPERIMENTAL SETUP

Our experiments were performed on a room-temperature atomic cesium cell with a length of 10 cm and a diameter of 2 cm, the vapor pressure is estimated to be 2×10^{-6} torr, and no buffer gas is present in the cell to prevent unwanted mixed-species collisions. The cesium atoms are excited by two linearly polarized fields with parallel polarization, as shown in Fig. 2. The pump beam is provided by an external cavity diode laser (Sacher TEC100, 100 mW), which produces a continuous wave (cw) at 852 nm, which is collimated into the cell. A mechanical chopper modulates the intensity of the pump beam at 1 kHz. The frequency of the pump laser is stabilized on a Doppler-free saturation absorption spectrum (DFSAS), and the detuning Δ_p is varied relative to the transition $|6\,^2S_{1/2}, F=4\rangle \leftrightarrow |6\,^2P_{3/2}, F=5\rangle$ using an acousto-optical modulator (AOM). The coupling beam, which is produced by a tunable cw Ti:sapphire laser (Coherent Autoscan 899-29) is collimated into a 5-mm-diameter beam that propagates in a direction opposite to that of the pump beam. The coupling beam is scanned across the $|6\,^2P_{3/2}, F=5\rangle \leftrightarrow |8\,^2S_{1/2}, F=4\rangle$ transition for each pump beam detuning. The transmission profile of the pump beam is monitored by a homemade transimpedance amplifier which converts the photocurrent generated by the sensitive infrared detector (Thorlabs FDS 100) into a voltage signal in photodetector 1 (PD1 in Fig. 2). The lock-in amplifier demodulates the converted voltage, which is then recorded on a personal computer (PC). A bare diode (SDL BA630, indicated as Cal) is frequency injection-locked to the hyperfine transition $|6\,^2S_{1/2}, F=4\rangle \leftrightarrow |6\,^2P_{3/2}, F=4\rangle$. The detected beam of the coupling field interacts with the injection-locked field in another cesium cell, and the transmission intensity of this injection-locked laser is monitored by PD2, supporting the calibration of both the coupling frequency and the pump beam signal as the coupling frequency is scanned. With the coupling laser on and tuned across the resonance of the upper transition, the induced atomic coherence modifies the absorption of the pump field.

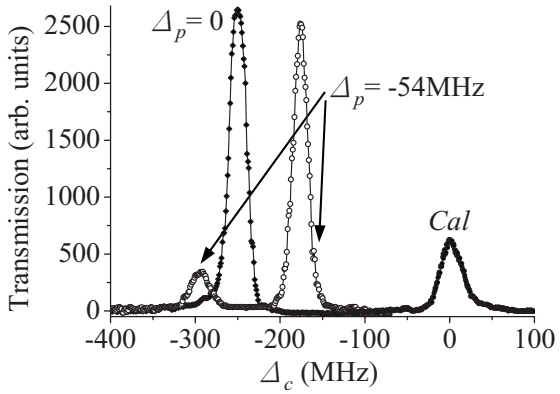

FIG. 3. Typical EIT spectrum with the calibration peak at the right. When $\Delta_p=0$, there is one distinct peak (diamonds). The EIT doublet appears when $\Delta_p=-54$ MHz (hollow circles). Cal: The calibration EIT peak.

III. RESULTS AND DISCUSSION

Figure 3 shows the measured pump beam transmission spectrum. As the coupling frequency is scanned with $\Delta_p=0$, one distinct transparency peak appears, corresponding to the $|6\,^2S_{1/2}, F=4\rangle \leftrightarrow |6\,^2P_{3/2}, F=5\rangle \leftrightarrow |8\,^2S_{1/2}, F=4\rangle$ resonance (diamond). The rightmost peak in Fig. 3 is the calibration peak, which corresponds to the same mechanism as the

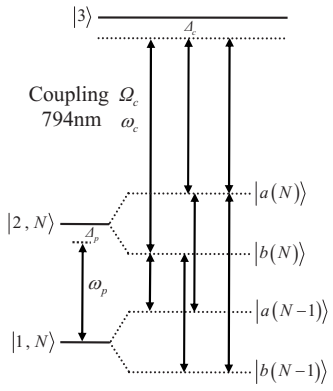

FIG. 4. Dressed state picture. The lower transition is further dressed by the pump field, and results in four possible transitions. The coupling field serves as the probe beam to probe each of the transitions to the higher state. Thus four sets of EIT configurations contribute.

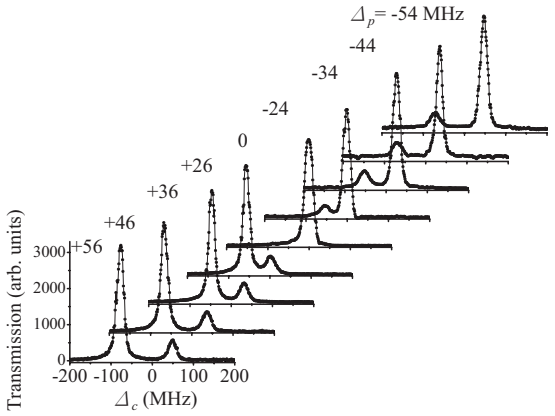

FIG. 5. Evolution of the EIT doublet. The increase of $|\Delta_p|$ enlarges the spacing of the EIT doublet, and varies the light shift of the center position, whereas the change of the sign of Δ_p alters the relative position of the EIT doublet.

above signal; this signal is on resonance with the transition $|6\ ^2S_{1/2}, F=4\rangle \leftrightarrow |6\ ^2P_{3/2}, F=4\rangle \leftrightarrow |8\ ^2S_{1/2}, F=4\rangle$. When the pump field is red detuned, $\Delta_p=-54$ MHz, two asymmetric peaks (hollow circles) are observed. The origin of the emergence of the two peaks can be interpreted in terms of the strongly driven Mollow structure of the lower transition. The plot clearly shows that the light shift that is caused by the ac Stark effect shifts the center of the two peaks relative to the central resonance corresponding to $\Delta_p=0$.

Figure 4 depicts this observation in detail. The initial uncoupled levels $|1,N\rangle$ and $|2,N\rangle$ contain information on the atomic bare states $|1,2\rangle$, and the average number of photons $\langle N\rangle$ in the laser mode. The condition $\langle N\rangle \to \infty$ must be satisfied to obtain a stationary result. The Hamiltonian of the lower transition is H_P+H_A, where

$$H_P = \hbar\omega_p\left(a^\dagger a + \frac{1}{2}\right) \tag{3}$$

is the Hamiltonian of the laser mode of the pump field, $a^\dagger$ and a are the creation and annihilation operators, and

$$H_A = 0|1\rangle\langle 1| + \hbar\omega_{12}|2\rangle\langle 2| \tag{4}$$

is the atomic Hamiltonian, based on the assumption that the eigenstates $|1,2\rangle$ have energies 0 and $\hbar\omega_{12}$, respectively.

In the strong pump driving scheme, the perturbed or the dressed states of the lower transition from Eqs. (3) and (4) are given by $|a(N)\rangle$, $|b(N)\rangle$, $|a(N-1)\rangle$, and $|b(N-1)\rangle$. The frequency spacing between these allowed transitions is

$$|b(N)\rangle \leftrightarrow |a(N-1)\rangle, \quad \omega_0 - \sqrt{\Delta_p^2+\Omega_p^2}, \tag{5a}$$

$$|b(N)\rangle \leftrightarrow |b(N-1)\rangle, \quad \omega_0, \tag{5b}$$

$$|a(N)\rangle \leftrightarrow |a(N-1)\rangle, \quad \omega_0, \tag{5c}$$

$$|a(N)\rangle \leftrightarrow |b(N-1)\rangle, \quad \omega_0 + \sqrt{\Delta_p^2+\Omega_p^2}, \tag{5d}$$

where ω_0 is the transition frequency of the central components [Eqs. (5b) and (5c)]. These transitions are further coupled by the coupling field to the higher state. Notably, the coupling beam serves as a "probe" beam to probe the dressed structures of the lower transition, but it also strongly drives the upper transition, so that the system is doubly dressed and in total constructs four sets of stepwise EIT transitions from the $|6\ ^2S_{1/2}, F=4\rangle$ to the $|8\ ^2S_{1/2}, F=4\rangle$ state.

However, when two-photon stepwise resonance occurs, the stimulated emission and absorption rates for the lower transitions are equal in Eqs. (5b) and (5c), and the manner of probing the Mollow structure to the higher state contributes an additional decay rate of Γ_3 to the transitions, possibly causing failure of the secular approximation [1]. These facts explain the vanishing of the central component and the fact that the two sidebands in Eqs. (5a) and (5d) are observed in the absorption spectra. Figure 5 shows the evolution of the line shape of the EIT doublet as Δ_p varies. Figure 5 includes three signatures. The first, the position of the maximum peak in relation to the position of the smaller peak, changes as the sign of Δ_p changes. The second, the center frequencies of both peaks, changes with the Δ_p value; this variation is the light shift that is presented in Fig. 3. The third, the splitting of the EIT doublet, widens as $|\Delta_p|$ increases. These characteristics closely match the Mollow spectrum [3]. Equations (5a) and (5d) clearly indicate that the frequency difference of the EIT doublet equals

$$2\sqrt{\Delta_p^2+\Omega_p^2}. \tag{6}$$

For a quantitative comparison, Fig. 6 plots the experimental frequency splitting of the EIT doublet as a function of Δ_p. The splitting of the EIT doublet is compared with the theoretical curve from Eq. (6). The theory and experiment agree reasonably closely with no free parameters. The interpolation of the theoretical curve yields the effective Rabi frequency of 17.56 MHz, which agrees closely with the estimate. Figure 7 plots the light shift deduced from the experimental points as a function of Δ_p. The plot exhibits considerable irregularity. The experimental line shape is considered with reference to Eq. (2) in Ref. [3], as shown in Fig. 8, to elucidate the strange behavior of the light shift. A large Δ_p regime was

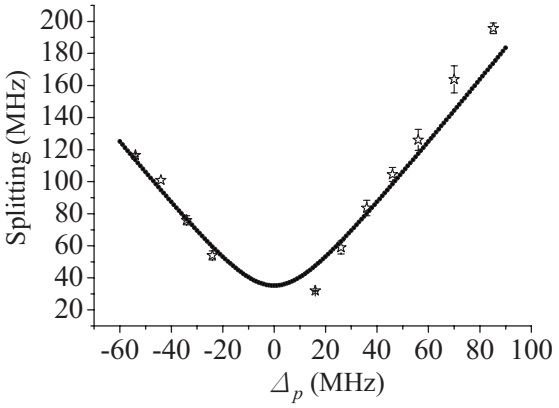

FIG. 6. Splitting of the EIT doublet as a function of Δ_p.

selected to satisfy the secular approximation. The solid curve represents the line shape without integration of the velocity group, and the amplitude of the absorption component is normalized to the maximum peak in the spectrum. The simulation demonstrates that the experimental linewidth is broader than the theoretical one. Moreover, the secondary peak of the experimental spectrum, which corresponds to the gain component of the Mollow spectrum, has a larger amplitude than that theoretically simulated. We posit that the difference is associated with the additional contribution from the transparency property due to the nature of EIT.

The dashed curve in Fig. 8 plots the simulated results when the Dopper velocity group is considered, so the detuning of the two fields is modified as

$$\Delta_p \rightarrow \Delta_p + \frac{\vec{V}}{c}\omega_p, \tag{7a}$$

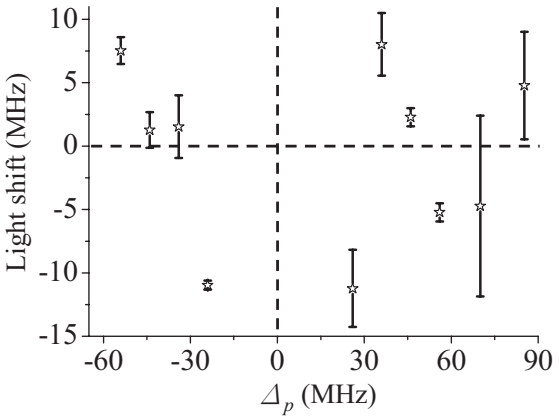

FIG. 7. Light shift of the center position corresponding to the singlet EIT peak at $\Delta_p=0$. The plot shows a messy distribution, and we attribute this phenomenon to the influence of the Doppler velocity group (see text).

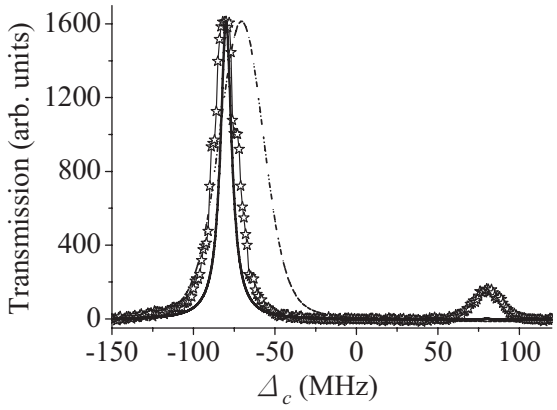

FIG. 8. Comparison of the experimental spectrum (stars) with the theoretical simulations with (dashed) or without (solid) integrating the Doppler velocity group. The simulation parameters are $\Gamma_2=5.22$ MHz, $\Gamma_3=2.18$ MHz, $\Omega_p=38$ MHz, $\Delta_p=70$ MHz, and the velocity distribution is integrated from −5000 to +5000 m/s.

$$\Delta_c \rightarrow \Delta_c - \frac{\vec{V}}{c}\omega_c, \tag{7b}$$

where c is the light speed, and $\vec{V}$ is the velocity of the cesium atoms in the laser beam propagation direction. The velocity distribution is summed over conventional Maxwell-Boltzmann statistics (at 300 K). The simulation indicates that Doppler averaging substantially broadens the observed spectrum and shifts the peak position, explaining why the abnormal light shift is induced mainly by the velocity group. However, these results also suggest that Doppler broadening was suppressed by the quantum interference between the transition pathways in the EIT scheme. Incorporating the above mechanism thus qualitatively explains the spectrum.

IV. CONCLUSIONS

Doubly dressed states were observed in a room-temperature atomic sample. The normal method for probing the strongly driven two-level system was not used. Rather, this work demonstrated the approach of elucidating the Mollow spectrum of the lower transition based on the EIT configuration, which is generated from the dressed state of the upper transition. The absorption and the gain components are observed and interpreted as the EIT doublet structure. The spacing of the EIT doublet is strongly consistent with the theoretical description of the Mollow spectrum, and the numerical simulation demonstrates that Doppler broadening can be greatly reduced using this detection technique. The simulation results also show that the Doppler velocity group can cause an exotic light shift. Experimental evidence shows that the dressed state approach offers a simple interpretation of the observed transparency multiples in the spectrum.

ACKNOWLEDGMENT

We wish to acknowledge the support of this work by the National Science Council, Taiwan.

[1] C. Cohen-Tannoudji and S. Reynaud, J. Phys. B **10**, 345 (1977).
[2] B. R. Mollow, Phys. Rev. **188**, 1969 (1969).
[3] F. Y. Wu, S. Ezekiel, M. Ducloy, and B. R. Mollow, Phys. Rev. Lett. **38**, 1077 (1977).
[4] S. H. Autler and C. H. Townes, Phys. Rev. **100**, 703 (1955).
[5] R. G. Brewer and E. L. Hahn, Phys. Rev. A **11**, 1641 (1975).
[6] T. Zanon, S. Guerandel, E. de Clercq, D. Holleville, N. Dimarcq, and A. Clairon, Phys. Rev. Lett. **94**, 193002 (2005).
[7] S. Harris, Phys. Today **50**(7), 36 (1997).
[8] M. Fleischhauer, A. Imamoglu, and J. P. Marangos, Rev. Mod. Phys. **77**, 633 (2005).
[9] A. Aspect, E. Arimondo, R. Kaiser, N. Vansteenkiste, and C. Cohen-Tannoudji, Phys. Rev. Lett. **61**, 826 (1988).
[10] S. E. Harris, Phys. Rev. Lett. **62**, 1033 (1989).
[11] T. Hong, C. Cramer, W. Nagourney, and E. N. Fortson, Phys. Rev. Lett. **94**, 050801 (2005).
[12] G. S. Agarwal and W. Harshawardhan, Phys. Rev. Lett. **77**, 1039 (1996).
[13] S. F. Yelin, V. A. Sautenkov, M. M. Kash, G. R. Welch, and M. D. Lukin, Phys. Rev. A **68**, 063801 (2003).
[14] S. E. Harris and Y. Yamamoto, Phys. Rev. Lett. **81**, 3611 (1998).
[15] H. Wang, D. Goorskey, and M. Xiao, Phys. Rev. Lett. **87**, 073601 (2001).
[16] J. Dalibard and C. Cohen-Tannoudji, J. Opt. Soc. Am. B **6**, 2023 (1989).
[17] P. R. Berman, B. Dubetsky, and J. Guo, Phys. Rev. A **51**, 3947 (1995).
[18] D. Kruse, C. von Cube, C. Zimmermann, and P. W. Courteille, Phys. Rev. Lett. **91**, 183601 (2003).
[19] G. R. M. Robb, N. Piovella, A. Ferraro, R. Bonifacio, Ph. W. Courteille, and C. Zimmermann, Phys. Rev. A **69**, 041403(R) (2004).
[20] D. R. Meacher, D. Boiron, H. Metcalf, C. Salomon, and G. Grynberg, Phys. Rev. A **50**, R1992 (1994).
[21] S. Inouye, A. P. Chikkatur, D. M. Stamper-Kurn, J. Stenger, D. E. Pritchard, and W. Ketterler, Science **285**, 571 (1999).
[22] M. Yan, E. G. Rickey, and Y. Zhu, Phys. Rev. A **64**, 013412 (2001).
[23] L. Yang, L. Zhang, X. Li, L. Han, G. Fu, N. B. Manson, D. Suter, and C. Wei, Phys. Rev. A **72**, 053801 (2005).
[24] S. Wielandy and A. L. Gaeta, Phys. Rev. A **58**, 2500 (1998).